© 2018. Published by The Company of Biologists Ltd | Development (2018) 145, dev164046. doi:10.1242/dev.164046

RESEARCH ARTICLE

Leukocyte receptor tyrosine kinase interacts with secreted midkine to promote survival of migrating neural crest cells

Felipe Monteleone Vieceli and Marianne E. Bronner*

ABSTRACT

Neural crest cells migrate long distances throughout the embryo and rely on extracellular signals that attract, repel and/or stimulate survival to ensure proper contribution to target derivatives. Here, we show that leukocyte receptor tyrosine kinase (LTK), an ALK-type receptor tyrosine kinase, is expressed by neural crest cells during early migratory stages in chicken embryos. Loss of LTK in the cranial neural crest impairs migration and results in increased levels of apoptosis. Conversely, midkine, previously proposed as a ligand for ALK, is secreted by the non-neural ectoderm during early neural crest migratory stages and internalized by neural crest cells *in vivo*. Similar to loss of LTK, loss of midkine reduces survival of the migratory neural crest. Moreover, we show by proximity ligation and co-immunoprecipitation assays that midkine binds to LTK. Taken together, these results suggest that LTK in neural crest cells interacts with midkine emanating from the non-neural ectoderm to promote cell survival, revealing a new signaling pathway that is essential for neural crest development.

KEY WORDS: Neural crest, LTK, Midkine, Cell survival, Apoptosis, Chicken

INTRODUCTION

The neural crest is a population of stem-like cells that emigrates from the dorsal neural tube and forms a vast array of derivatives in the vertebrate embryo. Neural crest cells not only contribute to the peripheral nervous system, but also to the craniofacial skeleton, parts of the cardiac outflow tract and all skin pigment cells (Green et al., 2015; Le Douarin and Kalcheim, 1999). Onset of neural crest migration begins with an epithelial-mesenchymal transition (EMT) that resembles the first steps of cancer metastasis: attachment between epithelial cells is lost and emigration proceeds with invasion of the basal extracellular matrix (Acloque et al., 2009; Kerosuo and Bronner-Fraser, 2012; Thiery et al., 2009).

Changes in cell shape and adhesive properties that occur during EMT enable detachment of neural crest cells and their subsequent migration through mesenchymal tissue (Rogers et al., 2013; Scarpa et al., 2015). A number of extracellular signals have been identified that interact with receptors present in the membrane of migrating neural crest cells to regulate their direction of migration, proliferation and survival; these include ErbB/neuregulin, Eph/Ephrin, neuropilin/semaphorin, CXCR4/SDF and VEGFR/VEGF (Kulesa and Gammill, 2010; Gammill et al., 2007; McLennan et al., 2010; Olesnicky Killian et al., 2009; Osborne et al., 2005; Schwarz et al., 2008; Theveneau et al., 2010; Theveneau and Mayor, 2012). In addition, cell adhesion molecules are crucial for many aspects of EMT and progression of cell migration. For example, EMT is accompanied by a switch in expression from type 1 (Ecad and Ncad) to type 2 (Cad7, Cad6b and Cad11) cadherins (Cheung et al., 2005; Dottori et al., 2001; Fairchild and Gammill, 2013; Kashef et al., 2009; Nieto et al., 1994; Taneyhill et al., 2007; Taneyhill, 2008; Vallin et al., 1998). In addition, Cad6B must be repressed for dissociation of neural crest cells from the neural tube (Coles et al., 2007) and Ecad is important for neural crest cell-cell adhesion during early migration in both chick and frog (Huang et al., 2016; Rogers et al., 2013). Some differences, however, exist between species: whereas maintenance of Ncad is important for contact inhibition of locomotion during migration in *Xenopus* and zebrafish (Bahm et al., 2017; Scarpa et al., 2015; Theveneau et al., 2010), Ncad is absent from migrating neural crest cells in chick, which instead express cadherin 7 (Rogers et al., 2018).

In an effort to identify novel signaling and adhesion molecules that may play a role during neural crest migration, we have performed transcriptional profiling of early migrating cranial neural crest cells (Simões-Costa et al., 2014). Among the genes uncovered, leukocyte receptor tyrosine kinase (LTK) was found to have a striking neural crest-specific expression pattern. LTK was first identified in cells of hematopoietic origin and later found to be required for proliferation and survival of iridophores in zebrafish embryos (Ben-Neriah and Bauskin, 1988; Fadeev et al., 2016; Lopes et al., 2008). However, the endogenous function of LTK during cell migration has been unclear. In chicken, LTK is more similar in structure to its better-known vertebrate paralog anaplastic lymphoma kinase (ALK), mutations of which result in pediatric neural crest-derived tumors of the sympathoadrenal lineage, the cell type in which ALK is first expressed (Hurley et al., 2006). The conserved extracellular region of ALK/LTK contains a low-density receptor class A repeat (LDLa) flanked by one or two meprim/A5 protein/PTPμ (MAM) domains and a glycine-rich region (GlyR), the conservation of the latter also extending to mammals. LTK and ALK were considered orphan receptors until the recent discovery that secreted proteins previously known as FAM150A/B bind to the GlyR domain (Guan et al., 2015; Reshetnyak et al., 2015; Zhang et al., 2014). As a result, these proteins were renamed as ALK and LTK ligand-1/2 (ALKAL1 and ALKAL2). Recently, both were shown to be required for formation of zebrafish iridophores, a process dependent on LTK activity (Lopes et al., 2008; Fadeev et al., 2016; Mo et al., 2017). However, the presence of other conserved domains in the extracellular region suggests that the full range of LTK and ALK ligands remains ill-defined. For example, it has been suggested that the heparin-binding cytokines midkine and pleiotrophin are ligands for ALK (Stoica et al., 2001, 2002), and midkine affects proliferation of sympathetic neurons in a manner thought to be ALK dependent (Reiff et al., 2011).

Division of Biology and Biological Engineering, California Institute of Technology, 1200 E California Boulevard, Pasadena, CA 91125, USA.

*Author for correspondence (mbronner@caltech.edu)

F.M.V., 0000-0001-5142-8224; M.E.B., 0000-0003-4274-1862

Received 6 February 2018; Accepted 13 September 2018

Development (2018) 145, dev164046. doi:10.1242/dev.164046

Here, we reveal a functional interaction between LTK and midkine during early neural crest migration. We find that chicken LTK is required for survival of migrating cranial neural crest cells, but not for neural crest identity. During early migration, cranial crest cells expressing LTK are in contact with the basal lamina of the non-neural ectoderm before moving ventrally. Our data show that midkine produced by the non-neural ectoderm accumulates in the basal lamina, binds to LTK and is internalized by neural crest cells, which require midkine for survival. This anti-apoptotic effect of LTK/midkine provides evidence for a new signaling pathway that is important for neural crest development.

RESULTS

LTK is expressed in migrating neural crest cells

As a first step in addressing the role of LTK during neural crest development, we examined its expression pattern at different embryonic stages. To this end, we performed whole-mount *in situ* hybridization on chicken embryos between Hamburger and Hamilton (HH) stages 4 and 19 (Hamburger and Hamilton, 1951). At HH4-5, corresponding to gastrula stages, *LTK* transcripts were solely detected in cells adjacent to the primitive streak, likely to be ingressing mesodermal cells (Fig. S1A,B). Expression in the neural crest was first observed in the dorsal neural folds of stage HH8+ embryos (Fig. 1A). By stage HH10, strong *LTK* signal was present in migrating cranial neural crest cells that co-expressed the HNK-1 antigen, as well as in pre-migratory cardiac/vagal neural crest cells (Fig. 1B-D). At stage HH14, *LTK* expression was already present in premigratory trunk neural crest cells and maintained during their migration at HH19 (Fig. 1E,F). At this later stage, *LTK* expression was detected in the trigeminal ganglia and in vagal and trunk neural crest migration streams (Fig. 1F,G).

Loss of LTK impairs cranial neural crest migration

To determine whether LTK is required in migrating neural crest cells, we performed loss-of-function experiments with a fluorescein (FITC)-tagged antisense splice-blocking morpholino oligo (MO) targeting the *LTK* exon 8/intron 8 junction by *ex ovo* electroporation of the ectoderm of late gastrula stage embryos (HH6). To confirm activity of the MO, we electroporated embryos with morpholinos and harvested RNA from stage HH8+ dorsal neural folds to analyze the splicing of the target region with RT-PCR. Sequencing of the products obtained revealed that LTK-targeted MO (LTK-MO) caused skipping of exon 8 and a reading frame shift, producing a premature stop codon that truncates translation of LTK at the MAM domain, whereas a FITC-tagged standard control morpholino (ctrl-MO) did not perturb splicing of LTK (Fig. S2A).

To study the effects of MO-mediated knockdown in migrating neural crest cells, we electroporated HH6 embryos with LTK-MO on the right side and ctrl-MO on the left side, thus providing an internal control. Embryos were incubated to stage HH9+ (8-9 somites), corresponding to the time when the cranial neural crest had just started emigrating from the neural tube, then fixed and immunostained for the neural crest transcription factor Pax7 (Fig. 2A). To assess the average distance migrated away from the neural tube, we measured the area occupied by the right-side and left-side migrating populations. The data show that neural crest populations transfected with LTK-MO spread across an area equivalent to, on average, 85.7% of controls (Fig. 2B-D,H).

To confirm the MO phenotype using a second approach, we used CRISPR/Cas9 plasmid constructs, previously optimized for electroporation of chicken embryos, to induce mutations in the *LTK* locus (Gandhi et al., 2017). For this purpose, we designed a guide RNA (gRNA) targeting exon 20 of *LTK* (LTK.20), with the goal of specifically disrupting translation of the intracellular kinase

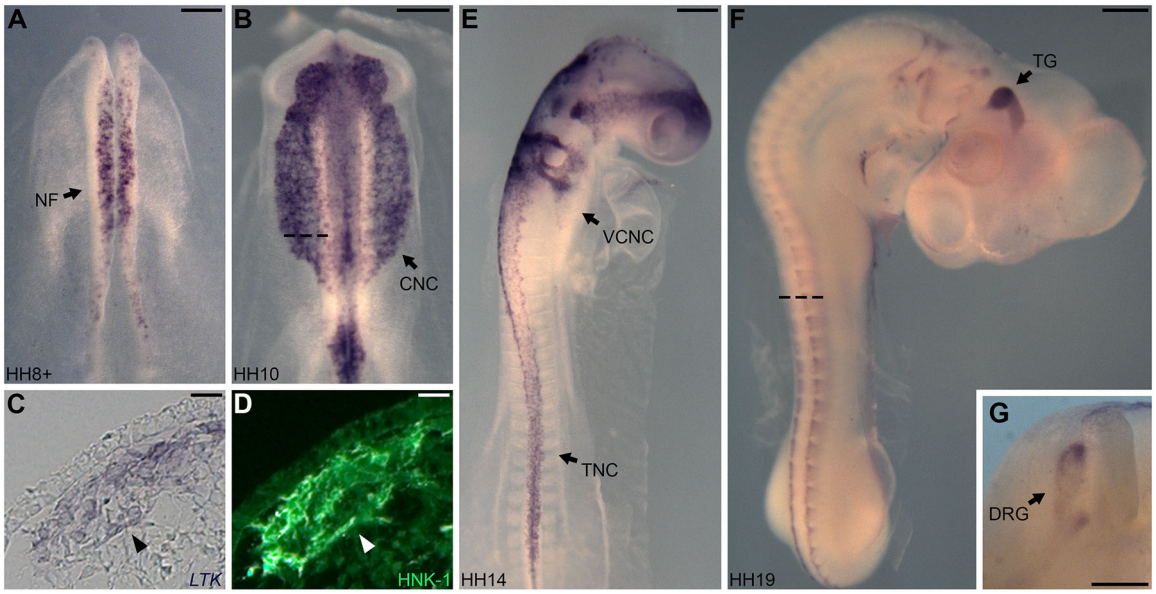

Fig. 1. *LTK* is expressed in migrating neural crest cells. (A) *In situ* hybridization showing *LTK* expression at stage HH8 in the dorsal neural folds (arrow) containing premigratory neural crest cells prior to neural tube closure. (B-D) At stage HH10, *LTK* transcripts are detected in migrating cranial neural crest cells (B, arrow) and overlapped with HNK-1 immunostaining in transverse sections (C,D, arrowheads), confirming their identity. (C,D) Transverse section of the region indicated by the dashed line in B. (E) At stage HH14, *LTK* expression is observed in later migrating cranial neural crest cells and in migrating and pre-migratory cardiac/vagal and trunk neural crest cells (arrows). (F) At stage HH19, *LTK* expression continues in migrating neural crest cells, trigeminal ganglia (arrow) and in cells located in the heart. (G) Transverse section of the region indicated by the dashed line in F, showing strong signal in dorsal root ganglia (arrow). CNC, cranial neural crest; DRG, dorsal root ganglia; NF, neural folds; TG, trigeminal ganglia; TNC, trunk neural crest; VCNC, vagal/cardiac neural crest. Scale bars: 200 µm in A,B,E; 20 µm in C,D; 500 µm in F; 100 µm in G.

Development (2018) 145, dev164046. doi:10.1242/dev.164046

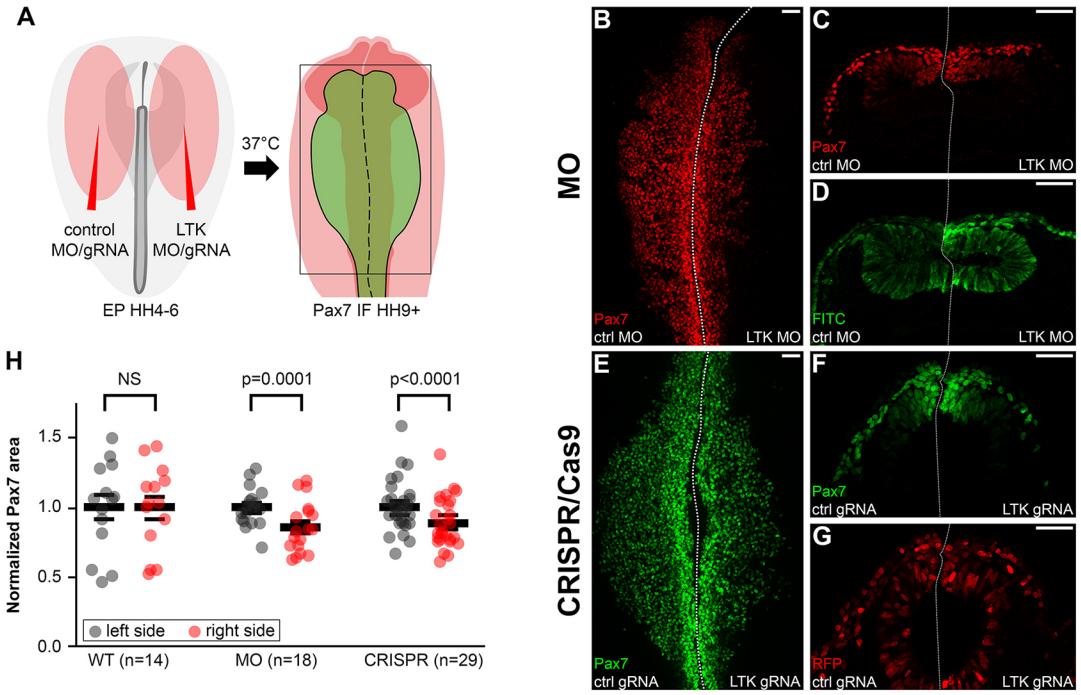

Fig. 2. Loss of LTK impairs cranial neural crest migration. (A) Diagram showing bilateral ectoderm electroporation of gastrula-stage chicken embryos with control reagents on the left side and LTK-targeted reagents on the right side, followed by *ex ovo* culture until stage HH9+. At this stage, dorsal view imaging of the neural crest allows area measurements suitable for comparing the average distance migrated. EP, electroporation; IF, immunofluorescence. (B) Immunostaining for Pax7 after MO-mediated unilateral depletion of LTK showing reduced migration on the right side. (C,D) Pax7 immunostaining (C) and MO FITC-tag signal (D) in a transverse section of the embryo shown in B. (E) Immunostaining for Pax7 after CRISPR/Cas9-mediated unilateral depletion of LTK showing reduced migration on the right side. (F,G) Pax7 immunostaining (F) and RFP signal (G) in a transverse section of the embryo shown in E. RFP reporter and Cas9 were electroporated on both sides (G). (H) Quantification of the Pax7 field areas in experimental and contralateral control sides showing significant decrease in the area spread by LTK-depleted neural crest, on average to 85.5% after MO treatment (n=18, P=0.0001) and 88.2% (n=28, P<0.0001) after CRISPR/Cas9 treatment. No significant difference (NS) was observed between the sides of wild-type (WT) embryos. The data are normalized to the left side average of each group and a two-tailed paired t-test was used to calculate statistical significance of the difference between left and right sides. Mean±s.e.m values are plotted as black bars. In this and subsequent figures, dotted line indicates midline. Scale bars: 50 µm.

domain at the carboxyl terminus without affecting membrane localization. To validate efficiency of this gRNA, we transfected a line of DF-1 chicken embryonic fibroblasts that constitutively expresses Cas9 (Gandhi et al., 2017) with LTK.20 driven by a chicken U6 promoter (cU6.3) and extracted genomic DNA after 48 h for PCR amplification followed by cloning and sequencing of the target region. Analysis of the data confirmed at least one deletion event on the target site that led to frameshift with a premature stop codon, validating the gRNA activity (Fig. S2B). This was a large deletion of 774 bp, suggesting that other CRISPR/Cas9-induced lesions at the LTK locus may not be readily accessible by routine detection methods (Kosicki et al., 2018). To knock down LTK in the neural crest, we electroporated CAG promoter-driven Cas9 and cU6.3-driven LTK.20 into the right side of HH4-5 embryos, together with pCI-H2B-RFP (Betancur et al., 2010) as a reporter. At the same time, a standard control gRNA was used in the left side as an internal control. Following transfection, the embryos were incubated until stage HH9+, then fixed and immunostained for Pax7. Analysis of the area occupied again indicated that LTK was required in migrating neural crest cells. On average, the populations transfected with LTK.20 occupied an area equivalent to 88.2% of contralateral control populations (Fig. 2E-H). Further supporting an LTK requirement, similar defects were observed after injection of the ALK/LTK pharmacological inhibitors ceritinib and crizotinib (Rodrigues et al., 2012) into the head mesenchyme of stage HH9 embryos (Fig. S3A-C), and after electroporation of pCI-H2B-RFP(V5-LTK-ΔICD), encoding an amino-terminal V5-tagged putative dominant-negative version of LTK that lacks the intracellular domain (LTK-ΔICD; Fig. S3D,E), designed in a similar fashion to previously described RTK dominant-negatives (Amaya et al., 1991; Saffell et al., 1997; Ueno et al., 1995).

To test whether loss of LTK alters neural crest specification, we performed immunostaining for Pax7 in MO-treated HH8 embryos, prior to neural tube closure and onset of migration, and observed no reduction in the neural crest population (Fig. 3A,B) or increased cell death (Fig. 3C), also excluding MO toxicity as a cause for the phenotype observed. We also stained HH10 embryos after MO- or CRISPR/Cas9-induced loss of LTK for neural crest markers *FoxD3*, *Ets1*, *Sox10*, Snail2 and Sox9, and found no obvious difference in their levels (Fig. 3D-H), suggesting that neural crest identity is not downstream of LTK. These markers, however, showed migration defects similar to Pax7 (Fig. 2H), where LTK-depleted Snail2$^+$ and Sox9$^+$ cells occupied on average an area equivalent of 89.7% and 80.3% of controls, respectively (Fig. 3I). We also observed no obvious effects in the expression of adhesion and extracellular matrix molecules associated with EMT, such as E-cadherin (Ecad), cadherin-6B (Cad6B) and laminin (Fig. S4). However, a reduction in the expression of the late migration marker HNK-1 suggested loss of neural crest cells during early migration (Fig. 3J).

LTK is required for survival of migrating neural crest cells

The results obtained with loss-of-function experiments might be due to defective cell migration and/or loss of neural crest cells.

Development (2018) 145, dev164046. doi:10.1242/dev.164046

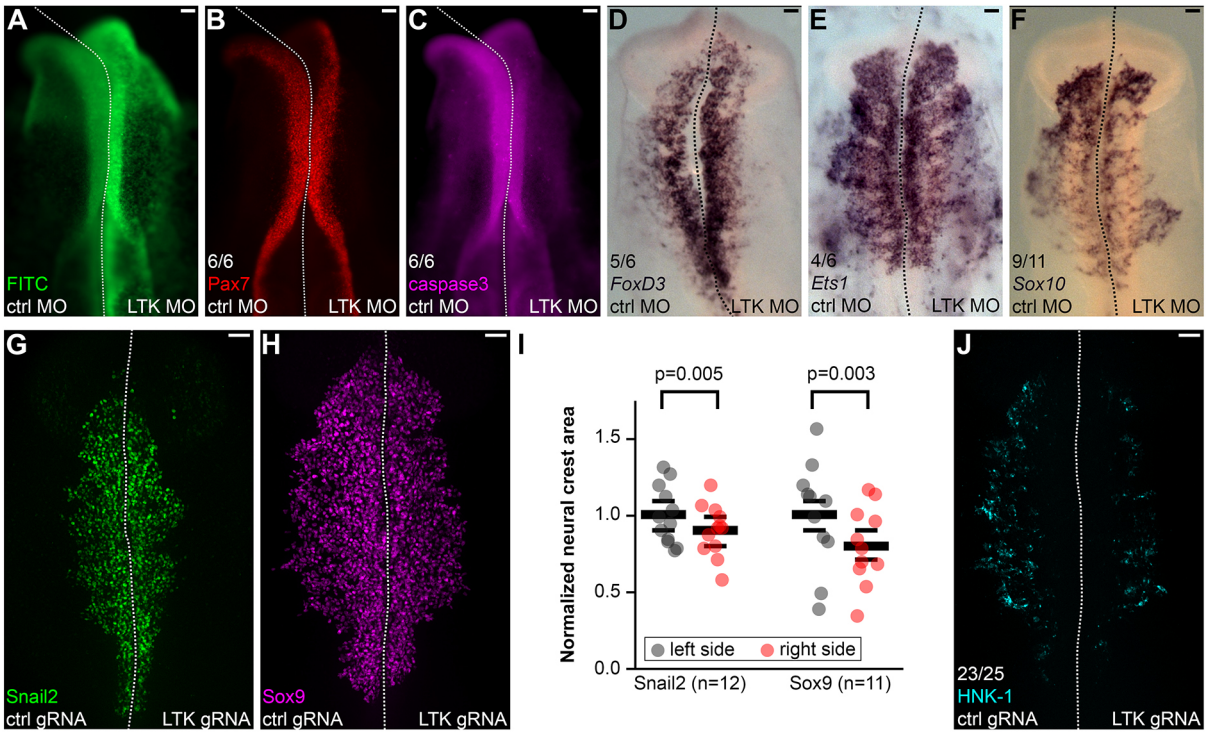

Fig. 3. LTK is not required for maintenance of neural crest identity. (A-C) Immunostaining of HH8 embryos after MO-mediated unilateral depletion of LTK (A) showing no obvious difference in levels of Pax7 (B) or cleaved caspase 3 (C) (6 out of 6 embryos). (D-F) *In situ* hybridization of HH10 embryos after MO-mediated unilateral depletion of LTK showing reduction in the average distance migrated on the right side but no obvious difference in expression levels of *FoxD3* (5 out of 6 embryos) (D), *Ets1* (4 out of 6 embryos) (E) and *Sox10* (9 out of 11 embryos) (F). (G,H) Immunostaining after CRISPR/Cas9-mediated unilateral depletion of LTK showing no obvious difference in Snail2 (G) and Sox9 (H) expression levels. (I) Quantification of the migratory neural crest area ratios between experimental and contralateral controls showing significant decrease in the average distance migrated by LTK-depleted neural crest, on average to 89.7% for Snail2 (n=12, P=0.005) and 80.3% for Sox9 (n=11, P=0.003). The data are normalized to the left side average of each group and a two-tailed paired t-test was used to calculate statistical significance of the difference between left and right sides. Mean±s.e.m. values are plotted as black bars. (J) Immunostaining after CRISPR/Cas9-mediated unilateral depletion of LTK showing reduction in HNK-1$^+$ late migratory neural crest cells at the right side (23 out of 25 embryos). Scale bars: 50 µm.

Besides the clear and reproducible reduction in the area occupied by neural crest cells, we also noted in transverse sections an apparent reduction in the number of migrating neural crest cells (Fig. 2E,G and Fig. 4A-D). To test whether this was correct, we counted the number of Sox9$^+$ cells after CRISPR-mediated loss of LTK. The results showed that depletion of LTK caused on average a reduction to 65.3% in the number of Sox9$^+$ cells compared with contralateral controls (Fig. 4E). Because onset of LTK expression takes place after neural crest specification and our results show that neither neural crest identity nor EMT were altered by its loss, this suggested that LTK function is important for ensuring proper size of the neural crest cell population, possibly by promoting cell survival. To test this possibility, we performed immunostaining for cleaved caspase 3, a marker for apoptotic cells. The results did indeed show increased levels of caspase 3-mediated apoptosis of early migrating neural crest cells transfected with CRISPR/Cas9 plasmids (Fig. 4F-J). These results confirmed that the phenotype observed was at least in part caused by increased cell death during migration. Increased signal for cleaved caspase 3 in the Pax7$^+$ migratory population after electroporation of LTK-ΔICD further supported these findings (Fig. S3E-G). Although we could not completely rule out an effect on cell migration as well, we found that LTK-depleted neural crest explants produced cells that migrated distances similar to cells from control explants (Fig. S5A,B,D,E), but also with higher levels of caspase 3-mediated apoptosis (Fig. S5C,F). Altogether, these data indicated that the main function of LTK is promoting cell survival during migration.

Midkine is expressed in the non-neural ectoderm juxtaposed to migrating neural crest cells

When screening full-length clones of chicken LTK obtained from stage HH10 cDNA, we identified two predominant variants. Interestingly, one of the isoforms lacked exon 16 and much of the glycine-rich region (GlyR) responsible for binding ALKAL1/2 in mammals and fish (Fig. S6) (Fadeev et al., 2018; Guan et al., 2015; Mo et al., 2017; Reshetnyak et al., 2015; Zhang et al., 2014). This raised the intriguing possibility that ligands other than ALKAL1/2 may bind to LTK during early neural crest migration. Moreover, a sequence homologous to *ALKAL1* in the chicken genome appears to have lost its function as there are no recognizable start and stop codons, and we did not detect *ALKAL2* expression in stage HH10 embryos by *in situ* hybridization (data not shown). Taken together, these observations suggest that other secreted molecules may be responsible for activating LTK at the stages examined.

To test this possibility, we used *in situ* hybridization to examine the expression of candidate ligands other than ALKAL1/2. Accordingly, heparin-binding cytokine midkine has been proposed as a ligand for ALK and functional studies in the chick embryo suggest that it activates ALK to regulate proliferation of sympathetic ganglia progenitors (Reiff et al., 2011). Therefore, we analyzed the expression of midkine transcripts during neural crest development. The results showed that midkine was highly expressed in the non-neural ectoderm of HH10 and HH20 embryos, immediately juxtaposed to migrating neural crest cells positive for HNK-1 (Fig. 5A-D). To characterize the localization of midkine

Development (2018) 145, dev164046. doi:10.1242/dev.164046

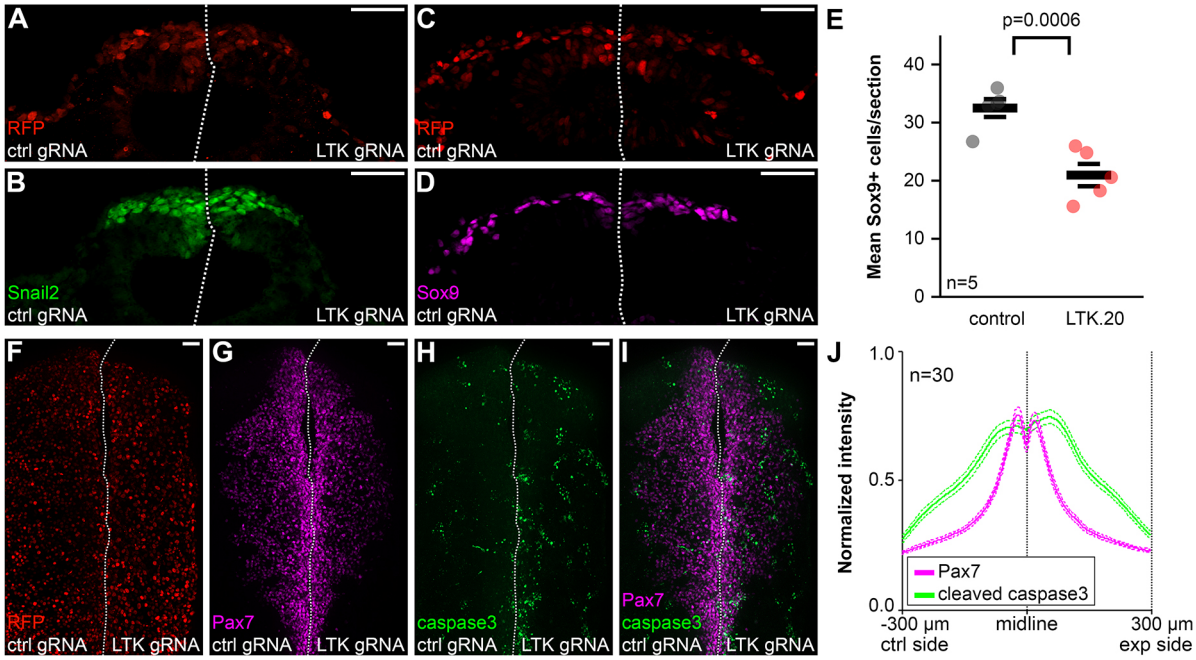

Fig. 4. LTK is required for neural crest survival. (A-D) Transverse sections of HH10 embryos immunostained for Snail2 (B) or Sox9 (D) after unilateral CRISPR/Cas9-mediated depletion of LTK showing reduced number of migrating neural crest cells at the right side. RFP reporter and Cas9 were electroporated on both sides (A,C). (E) Quantification of Sox9^{+} cell count ratios between experimental and contralateral controls obtained from transverse sections showing reduction of the number of cells in LTK-depleted neural crest populations on average to 65.3% (n=5, P=0.0006). The mean cell count per section for each embryo side is plotted and a two-tailed paired t-test was used to calculate statistical significance of the difference between left and right sides. Mean±s.e.m. values are plotted as black bars. (F-I) Immunostaining for cleaved caspase 3 after unilateral CRISPR/Cas9-mediated depletion of LTK showing increased number of apoptotic cells (H) amongst the Pax7^{+} population (G,I). RFP reporter and Cas9 were electroporated on both sides (F). (J) Profile of normalized mean fluorescence intensities acquired from dorsal view images (n=30) at equidistant positions from the midline showing increased levels of cleaved caspase 3 in the LTK-depleted side. Mean±s.e.m. values are plotted as dashed lines. Scale bars: 50 µm.

protein, we validated a commercial antibody with western blotting (Fig. S7E). Subsequent immunostaining of embryos revealed the presence of midkine in the basal lamina of the non-neural ectoderm (Fig. 5E,F), as expected based on transcript expression. Additionally, midkine protein was detected in the basal lamina of the neuroepithelium (Fig. 5F), likely remaining from earlier expression at the neural plate prior and during neurulation (Fig. S7A-D) similar to *mdk2* (*mdkb*) in zebrafish (Winkler and Moon, 2001; Winkler et al., 2003). Interestingly, we observed midkine signal around Pax7^{+} and HNK-1^{+} cells (Fig. 5G,H), suggesting that midkine signals secreted by the surface ectoderm into the extracellular matrix juxtaposing neural crest cells may be received by the latter. This is consistent with an interaction with membrane receptors of neural crest cells.

Loss of midkine impairs neural crest migration

If midkine is indeed a ligand for LTK, reducing its levels should phenocopy LTK loss of function and cause increased cell death. To test this, we inhibited production of midkine using a protein-based CRISPR/Cas9 electroporation strategy (Hutchins and Bronner, 2018), in order to circumvent early expression at the neural plate. To this end, we electroporated purified Cas9 protein and an *in vitro* synthesized gRNA targeting the first exon of midkine (MK.1) into the right side of the embryonic ectoderm after neural crest specification but before neurulation, whereas a control gRNA was electroporated into the left side. Embryos were allowed to develop until stage HH9+ (Fig. 6A,F), then fixed and immunostained for midkine, Pax7, HNK-1, Snail2, Ecad, Cad6B and cleaved caspase 3. This intervention resulted in a significant loss of midkine protein, validating activity of MK.1 (Fig. S7F-H). Depletion of midkine produced defects similar to LTK knockdown in the migratory population, as seen by Snail2, Pax7 and HNK-1 immunostaining (Fig. 6B,G,H), with an average reduction of the area occupied by Snail2^{+} and Pax7^{+} cells to 71.5% and 75.4%% of controls, respectively (Fig. 6K). Staining for cleaved caspase 3 revealed a dramatic increase in the numbers of apoptotic cells (Fig. 6I,L) amongst the migratory population (Fig. 6J), supporting a survival function for midkine. No obvious EMT defects were seen by analyzing expression of Ecad and Cad6B (Fig. 6C-E). These results showed that midkine prevents apoptosis of neural crest cells in a similar manner to LTK, consistent with a biologically relevant interaction.

Secreted midkine is internalized and promotes survival of neural crest cells

It has been reported that, upon binding to receptor, midkine is internalized by cells, a common phenomenon in RTK signaling (Marmor and Yarden, 2004). Thus, if midkine produced by the surface ectoderm binds to LTK in the migratory neural crest, one might expect to find secreted molecules inside the latter cell population. To investigate this possibility, we electroporated the non-neural ectoderm of stage HH9 embryos with pCI-H2B-RFP(midkine-FLAG) to express a CAG-driven carboxy-terminal FLAG-tagged form of midkine (Fig. 7A). Interestingly, 10 h post-electroporation, we observed FLAG signal within many Sox9^{+} migrating neural crest cells, despite the fact that the electroporation was confined to the non-neural ectoderm (Fig. 7B-D). The results suggest that midkine was secreted by the surface ectoderm and internalized by migrating neural crest cells.

Development (2018) 145, dev164046. doi:10.1242/dev.164046

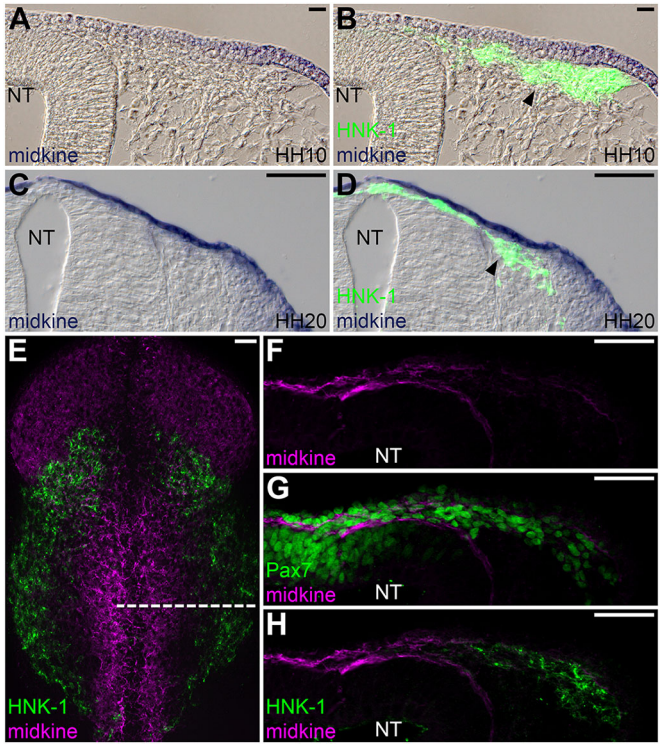

Fig. 5. Midkine is expressed in the non-neural ectoderm and accumulates in the basal lamina. (A-D) Transverse sections of the head of HH10 (A,B) or trunk of HH20 (C,D) embryos obtained after *in situ* hybridization combined with immunostaining showing expression of midkine transcripts in the non-neural ectoderm (A,C) that overlies migrating neural crest cells (arrowheads) stained for HNK-1 (B,D). (E) Immunostaining for midkine and HNK-1 in the head region of an HH10 embryo. (F-H) Transverse section of the embryo in E at the level of the dashed line showing protein accumulation in the basal lamina (F) and around Pax7$^+$ (G) and HNK-1$^+$ (H) neural crest cells. NT, neural tube. Scale bars: 50 µm.

To confirm that the staining detected originated from secreted midkine, we repeated this experiment using pCI-H2B-RFP(midkine-ΔSP-FLAG), which drives expression of midkine-FLAG lacking the signal peptide, encompassing the first amino-terminal 25 amino acids (midkine-ΔSP) and thought to be important for secretion. As expected, midkine-ΔSP remained inside transfected cells in the surface ectoderm and was not observed around or inside neural crest cells as was the case for full-length midkine (Fig. 7E-H), confirming the importance of the signal peptide for secretion. These results demonstrate that midkine secreted by the non-neural ectoderm is taken up and internalized by neural crest cells.

Midkine interacts with LTK

To test whether midkine and LTK interact *in vivo*, we performed a proximity ligation assay (PLA). This method allows specific protein-protein interactions to be detected *in situ* by secondary antibodies conjugated to unique short DNA strands that hybridize to allow a polymerase reaction that produces fluorescent signal when targets are within ∼40 nM of distance (Söderberg et al., 2006). To this end, we constructed pCAG(V5-LTK) and pCAG(V5-LTK-isoform2), encoding CAG-driven V5-tagged constructs of both LTK isoforms at the amino terminus of the mature protein, after signal peptide cleavage. Next, we used *ex ovo* electroporation to overexpress V5-LTK on the right side of stage HH5 embryos, whereas pCI-H2B-RFP was electroporated on both sides to allow use of cells on the left side as internal controls. For PLA, the embryos were fixed at stage HH9/10 and processed for cryosectioning. Immunostaining for V5 and midkine in adjacent transverse sections confirmed presence of both target proteins in the material used for PLA, and validated LTK localization at the cell membrane (Fig. 8A,B,G). In sections subjected to PLA with the same primary antibodies against V5 and midkine, we identified fluorescent puncta indicative of interaction events specifically around cells transfected with the canonical LTK isoform on the right side, whereas only occasionally puncta were observed on cells on the control side (Fig. 8C,D). Quantification of puncta across several sections confirmed a significant enrichment of interaction events in V5-LTK$^+$ side of the sections analyzed (Fig. 8E). These results strongly indicate that midkine binds to LTK and are consistent with a receptor-ligand interaction. Furthermore, the signal yielded by LTK isoform 2 (Fig. 8H,I), lacking most of the GlyR domain, indicates that this region is not required for interaction with midkine as it is for interaction with ALKAL1/2 (Reshetnyak et al., 2015). To confirm these results with an alternative approach, we transfected NIH/3T3 mouse fibroblasts with pCI-GFP(midkine-FLAG) and pCI-H2B-RFP(V5-LTK) to perform co-immunoprecipitation experiments. We detected both proteins in precipitates obtained after incubation with an anti-FLAG antibody, demonstrating that LTK and midkine bind to each other (Fig. 8F). Interestingly, only the uppermost band seemed to have been co-immunoprecipitatied with midkine, suggesting specific association with post-translationally modified LTK, which would be expected if midkine is a ligand.

If midkine does bind to LTK extracellularly, one would expect high affinity even in the absence of the intracellular domain. In fact, PLA performed with V5-LTK-ΔICD produced robust signal for interaction events (Fig. 8J-L). An amino-terminal V5-tagged construct lacking the extracellular domain (V5-LTK-ΔECD) also produces some signal after PLA, albeit at much reduced levels despite the similar construct size, which should confer comparable transfection efficiency (Fig. 8M-O). Altogether, these data strongly suggest that midkine is a survival factor that interacts with the extracellular region of the LTK receptor to promote cell survival.

DISCUSSION

During their migratory phase, neural crest cells move in tightly coordinated streams, with the number of cells and levels of proliferation in each influencing the contribution and ultimately the size of derived structures. Given that cell proliferation during migration is limited (Kulesa et al., 2010), neural crest cells must rely on mechanisms that ensure survival before and after colonization of their target sites. Here, we describe a novel mechanism that promotes survival of migrating cranial neural crest cells in the chick embryo.

It has been proposed that, upon EMT and detachment from the extracellular matrix, cells are exposed to different environments and have to adapt to ensure survival during migration (Frisch and Francis, 1994). Multiple lines of evidence suggest that biochemical signals are required to protect migrating neural crest cells from apoptosis. For example, neural tube cells forced to delaminate after RhoB or Ets1 overexpression undergo apoptosis, and Sox9-driven delamination rescues survival after RhoB overexpression, indicating that Sox9 is required for survival (Cheung et al., 2005). HoxB5 is likely to function upstream of Sox9, as perturbation of its signaling resulted in Sox9 downregulation and increased apoptosis (Kam et al., 2014). Similarly, inhibition of $\alpha_4\beta_1$ integrin receptor causes cell death of neural crest cells *in vitro* (Testaz and Duband, 2001),

Development (2018) 145, dev164046. doi:10.1242/dev.164046

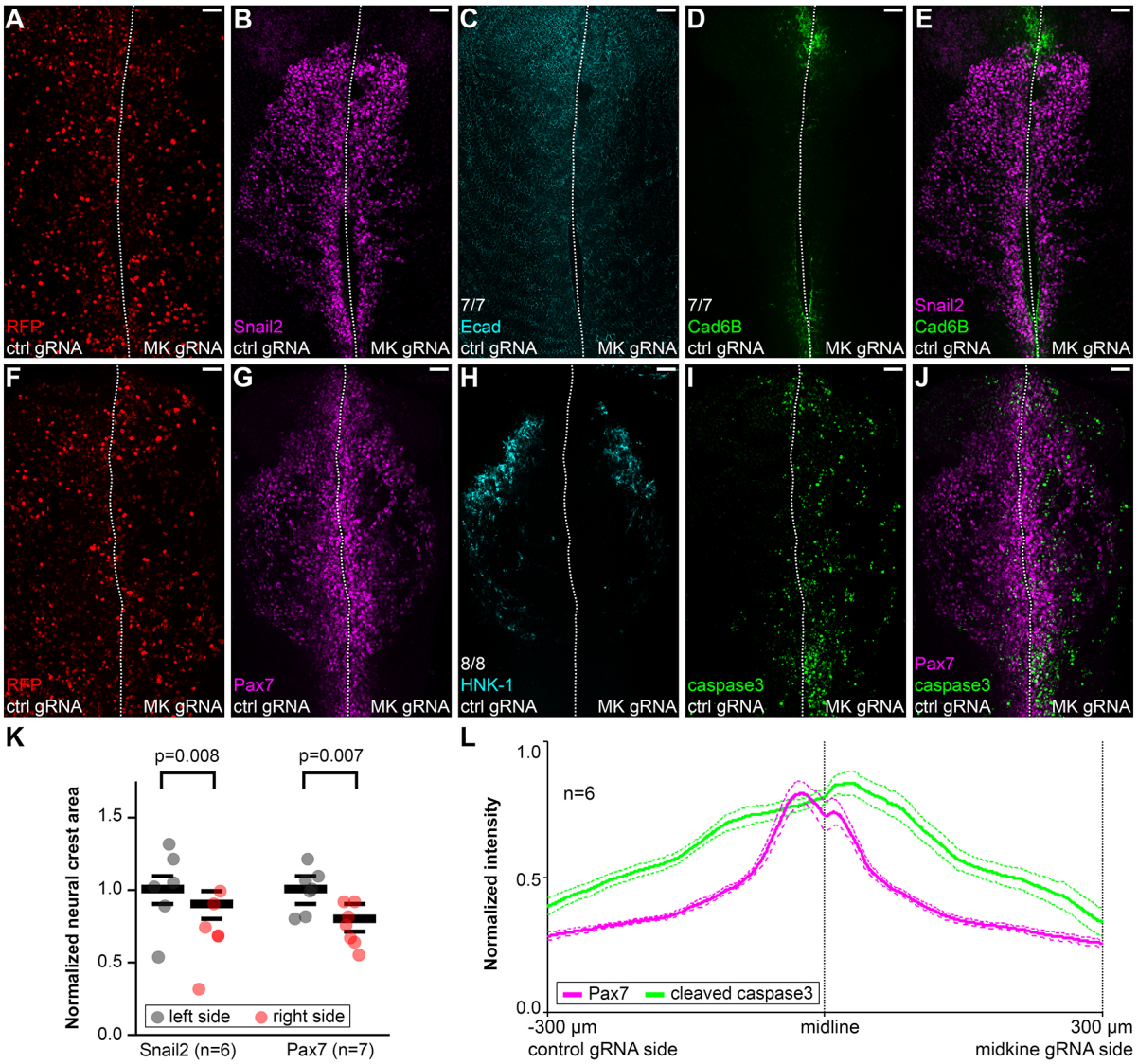

Fig. 6. Midkine is required for neural crest survival, but not maintenance of specification. (A-J) Immunostaining of HH10 embryos following unilateral loss of midkine mediated by CRISPR/Cas9 targeted by midkine (MK) gRNA (A,F) showing impaired migration with no loss of Snail2 (B,E) or Pax7 (G,J) expression, reduction in HNK-1^{+} late migratory population (8 out of 8 embryos) (H) and increased levels of cleaved caspase 3 levels (I,J), with no obvious effects in the expression of Ecad (7 out of 7 embryos) (C) or Cad6B (7 out of 7 embryos) (D,E). (K) Quantification of the migratory neural crest area ratios between experimental and contralateral controls showing significant decrease in the average distance migrated in the midkine-depleted side, on average to 71.5% for Snail2 (n=6, P=0.008) and 75.4% for Pax7 (n=7, P=0.007). The data are normalized to the left side average of each group and a two-tailed paired t-test was used to calculate statistical significance of the difference between left and right sides. Mean±s.e.m. values are plotted as black bars. (L) Profile of normalized mean fluorescence intensities acquired from dorsal view images (n=6) at equidistant positions from the midline showing increased levels of cleaved caspase 3 in the midkine-depleted side. Mean±s.e.m. values are plotted as dashed lines. Scale bars: 50 µm.

and antibody-mediated inhibition of sonic hedgehog ligands or conditional knockout of smoothened result in death of neural crest cells that colonize the branchial arches (Ahlgren and Bronner-Fraser, 1999; Jeong et al., 2004). In zebrafish, *tfap2a* is required for survival of preotic and postotic neural crest cells that migrate to the pharyngeal region (Barrallo-Gimeno et al., 2004). Moreover, anti-apoptotic roles of neural crest transcription factors are crucial for survival in premigratory stages: for example, antisense morpholino-mediated depletion of Sox10 or Id3 in *Xenopus* embryos results in increased apoptosis of neural crest progenitor cells (Honoré et al., 2003; Light et al., 2005; Kee and Bronner-Fraser, 2005) and Snail factors act in both neural crest and cancer cells in part by conferring resistance to apoptosis (Tríbulo et al., 2004; Nieto, 2002; Vega et al., 2004).

Our data suggest that the interaction between midkine and LTK is also crucial for proper neural crest survival during migration, as reduced levels of either receptor or ligand result in migration defects and cell death. This is consistent with previous *in vitro* data suggesting migration and survival activities for both midkine and LTK in cell lines (Kadomatsu and Muramatsu, 2004; Roll and Reuther, 2012; Qi et al., 2000; Tong et al., 2007; Ueno et al., 1996, 1997; Yao et al., 2010; Zou et al., 2006). Recently, the activating mutation on human ALK residue 1174 (ALK-F1174L), frequent in neuroblastoma, was shown to have a strong survival effect on cultured sympathetic neuroblasts, suggesting that a survival function could help explain the bad prognosis associated with excessive ALK signaling (Kramer et al., 2016). Although in zebrafish LTK seems to be required only in the neural crest derived

Development (2018) 145, dev164046. doi:10.1242/dev.164046

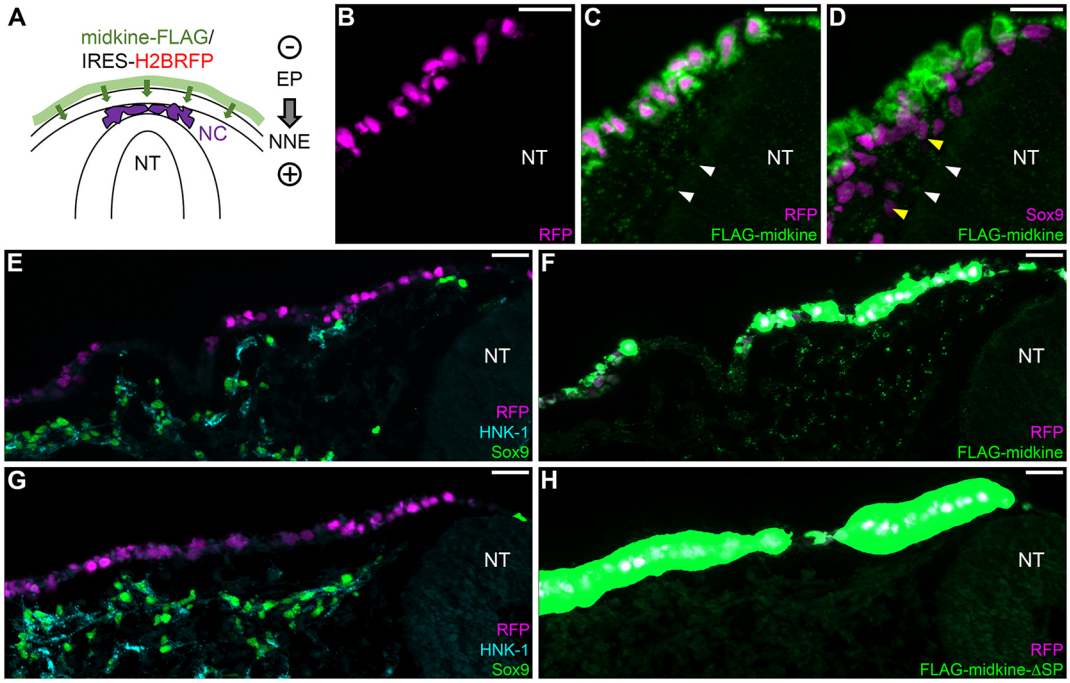

Fig. 7. Secreted midkine is internalized by migrating neural crest cells. (A) Diagram showing *in ovo* electroporation (EP) of the surface ectoderm from a transverse section view. Downwards transfection is restricted to the non-neural ectoderm cell layer (NNE) and does not reach the neural crest (NC) underneath. (B-D) Immunostaining of a transverse section through the embryonic head 10 h post-electroporation of midkine-FLAG showing RFP transfection confined to the non-neural ectoderm (B) and secreted midkine-FLAG speckles in the underlying mesenchyme (white arrowheads) (C), including the vicinity of non-transfected neural crest cells nuclei marked by Sox9 (yellow arrowheads), suggestive of internalization (D). (E-H) Immunostaining of a transverse section showing comparison of FLAG-tagged full-length midkine speckles secreted into the mesenchyme by the transfected ectoderm (5 out of 5 embryos) (F) versus a FLAG-tagged construct lacking the signal peptide (midkine-ΔSP) that remained inside the transfected cells (3 out of 3 embryos) (H). Exposure levels were kept constant in both samples for purposes of comparison and in high levels to best reveal the mesenchyme midkine-FLAG signal. NT, neural tube. Scale bars: 20 µm.

population of iridophores, and is also important for their survival (Fadeev et al., 2016), our data indicates that LTK has a broader requirement in the neural crest of avian species. Studies in other species will help understand the conservation of LTK requirement in the neural crest.

Recently, ligands for the ALK/LTK GlyR domain have been identified (Fadeev et al., 2018; Guan et al., 2015; Mo et al., 2017; Reshetnyak et al., 2015; Zhang et al., 2014). Although the GlyR domain seems to be only major recognizable extracellular domain in LTK that is conserved in mammals, all ALK proteins and non-mammalian LTK possess a conserved NMLM region as well, composed of an LDLa and one or two MAM domains (Lopes et al., 2008; Roll and Reuther, 2012). Proteins that bind these extracellular domains, however, remain unknown. The ligand for the LTK/ALK ortholog in *Drosophila* is the LDLa domain-containing ligand *jelly belly* (*jeb*), but an obvious ortholog is absent from vertebrate genomes (Lee et al., 2003; Weiss et al., 2001). After the first reports implicating midkine/pleiotrophin as ligands for ALK (Stoica et al., 2001, 2002), different groups failed to replicate activation of ALK by either putative ligand, placing the existence of these interactions in question (Dirks et al., 2002; Hugosson et al., 2014; Mathivet et al., 2007; Miyake et al., 2002; Moog-Lutz et al., 2005; Motegi et al., 2004; Mourali et al., 2006; Müller-Tidow et al., 2005). In contrast, our data are consistent with a ligand-receptor interaction. First, absence of significant ALKAL expression during early chicken development suggests that LTK signaling in early migrating neural crest cells depends on a distinct ligand. Second, using highly specific assays for detection of protein-protein interactions, we present the first evidence that LTK physically interacts with midkine *in vivo* and co-immunoprecipitates with midkine *in vitro*. Finally, similarity of LTK and midkine loss-of-function phenotypes and internalization of midkine by neural crest cells strongly support a ligand-receptor relationship. Our data also suggests that LTK is later downregulated in trunk neural crest cells as they differentiate into sympathoadrenal precursors, at which time they upregulate ALK, which is then required for midkine activity (Hurley et al., 2006; Reiff et al., 2011). In a different situation, midkine has been shown to confer resistance to cannabinoid anti-tumoral activity in glioma cells and block autophagy-mediated cell death specifically through activation of ALK, but not via other receptors previously described, such as LRP1 and PTPRZ (Lorente et al., 2011a,b). Altogether, these data strongly support a direct ligand-receptor interaction between ALK/LTK and midkine. However, given the resolution limit of PLA (~40 nM) signal production when using the secondary antibodies approach, our results could also be explained by interaction within a multiprotein complex. Consistent with this possibility, ALK becomes auto-phosphorylated upon binding of midkine dimers to an integrin/LRP complex (Muramatsu, 2010). The requirement of additional binding partners to mediate interaction between midkine and ALK/LTK may help explain the conflicting results in the literature.

Consistently associated with ALK and LTK activation, the ERK/MAPK signaling pathway is a likely intracellular effector of LTK survival activity (Fadeev et al., 2018; Roll and Reuther, 2012). Our data suggest that expression of Snail2 or Sox9 (Cheung et al., 2005; Tríbulo et al., 2004), neural crest transcription factors known to promote neural crest survival, is not dependent on LTK, indicating the existence of different transcriptional effectors of LTK function.

Development (2018) 145, dev164046. doi:10.1242/dev.164046

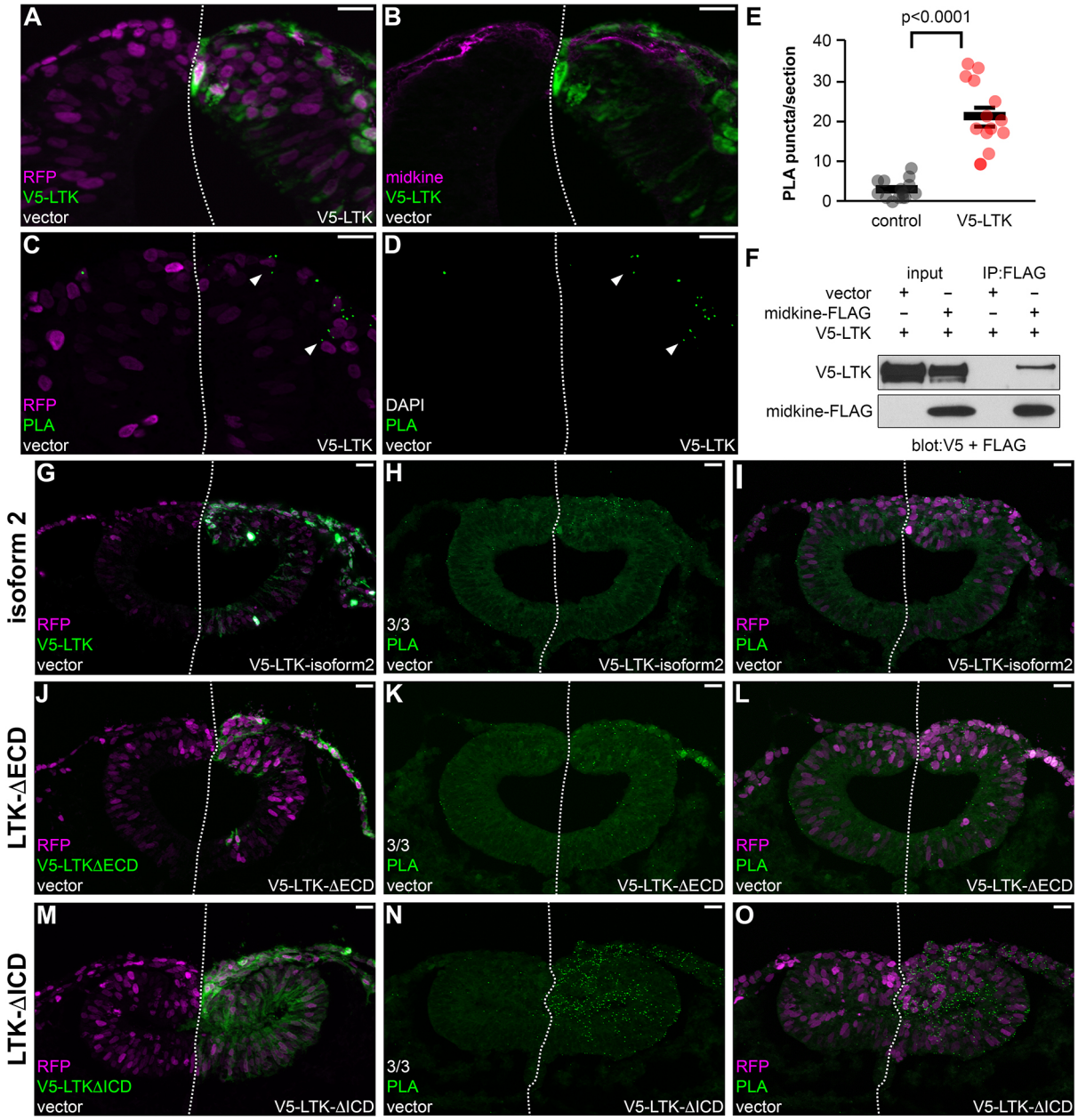

Fig. 8. Midkine and LTK bind extracellularly. (A,B) Immunostaining of a transverse section after unilateral ectopic expression of V5-LTK showing efficacy of anti-V5 and anti-midkine antibodies used for PLA and membrane localization of V5-LTK. (C,D) PLA performed in adjacent sections of the same embryo shown in A,B produces puncta (arrowheads) indicative of protein-protein interaction events (D) predominantly around the right-side RFP^+ cells (C). (E) Quantification of PLA puncta across several sections of two embryos showing enrichment on average to 7.2-fold (n=14, P<0.0001) at the V5-LTK side. The data for each section are plotted and a two-tailed paired t-test was used to calculate statistical significance of the difference between left and right sides. Mean±s.e.m. values are plotted as black bars. (F) Western blotting after anti-FLAG co-immunoprecipitation of lysates from mouse NIH/3T3 cells transfected with V5-LTK and an empty vector (pCI-GFP) or midkine-FLAG showing presence of V5-LTK only in the midkine-FLAG sample. (G-O) PLA experiments after unilateral ectopic expression verified with immunostaining (G,J,M) also produce positive signal for LTK isoform 2 (3 out of 3 embryos) (H,I), LTK-ΔECD (3 out of 3 embryos) (K,L) and LTK-ΔICD (3 out of 3 embryos) (N,O), with the latter exhibiting dramatically higher levels. RFP transfection reporter was electroporated on both sides (A,C,G,I,J,L,M,O). Gamma adjustments were performed in order to improve visualization of medium intensity levels of RFP and V5 staining (A-C,G,I,J,L,M,O). Scale bars: 20 µm.

Although we have not investigated which factors mediate LTK survival activity intracellularly, other candidates are the pro-apoptotic factors BMF and BIM, found to be downregulated by constitutively active ALK-F1174L (Kramer et al., 2016). Further characterization of the pathways downstream of LTK will be key for understanding the full mechanism of LTK action in migrating neural crest cells.

Cumulatively, our results show that neural crest cells start expressing the LTK receptor immediately prior to delamination and subsequently encounter a midkine-rich intercellular environment at early stages of migration. We show that midkine binds to LTK and is internalized by LTK-expressing neural crest cells. In the absence of either receptor or ligand, neural crest cells undergo apoptosis. Thus, we propose that secreted midkine binds to the extracellular region of LTK present in the membrane of neural crest cells to trigger intracellular transduction pathways that promote survival and migration, potentially as an activating ligand. We further speculate

Development (2018) 145, dev164046. doi:10.1242/dev.164046

that interactions between midkine and LTK function to maintain the proper number of neural crest cells within a migratory stream. This is consistent with findings in chick embryos where implanting additional neural crest cells leads to regulation of cell number, such that neural crest derivatives maintain their normal size (Baker et al., 1997). This results in matching of cell numbers to the size of derivatives via signaling events emanating from the environment. Taken together, our data provide a framework for understanding how midkine stimulates ALK-type receptors to trigger downstream pathways involved in cell survival.

MATERIALS AND METHODS

Embryos and electroporation

Fertilized *Gallus gallus* eggs were obtained from McIntyre Poultry & Eggs (Lakeside, CA, USA) and AA Lab Eggs (Westminster, CA, USA). The eggs were incubated at 37°C and embryos at the desired stage were collected as described (Chapman et al., 2001) and staged according to Hamburger and Hamilton (1951). Gastrula-stage HH4 to HH6 embryos were electroporated *ex ovo* (Sauka-Spengler and Barembaum, 2008) with five 50-ms pulses of 5.2-5.4 V spaced by 100-ms intervals and cultured until reaching HH8 to HH10 at 37°C. For electroporation of the non-neural ectoderm, HH9 (8 somites) embryos were electroporated *in ovo* (Itasaki et al., 1999) with five 50-ms pulses of 18 V spaced by 100-ms intervals and re-incubated for 10 h at 37°C. Embryos efficiently electroporated, based on FITC or RFP signal, were selected for downstream analysis.

Morpholino treatments

FITC-tagged standard control morpholino or splice-blocking morpholino targeted to *LTK* exon8/intron8 junction (LTK-MO: CAGAGGGAGAT-ACCTGGTAATCTTC) were electroporated at 0.5 mM. Injection solutions were complemented with 1 µg/µl carrier DNA (empty pTK-EGFP; Uchikawa et al., 2003). For activity validation, RNA samples isolated from neural folds of embryos electroporated with LTK-MO (n=2) or ctrl-MO (n=2) were reverse-transcribed with Superscript IV (Thermo Fisher Scientific) and subjected to RT-PCR with the primers LTK-F1/LTK-R1 (Table S1). The PCR products were cloned into pGEM-T (Promega) and sequenced.

CRISPR/CAS9-induced mutagenesis

Plasmids pCAG(Cas9) and cU6.3 driving expression of standard control (Gandhi et al., 2017) or targeted gRNAs were electroporated into HH4-5 embryos. A template for a gRNA targeting *LTK* exon 20 (LTK.20: GCAGAGAGATGTTCTTCCGT) was cloned into a *Bsa*I-digested cU6.3 backbone vector after annealing single-strand oligos to form compatible double-strand DNA. For LTK.20 validation, immortalized DF-1 chicken embryonic fibroblast cells (ATCC, CRL-12203, RRID:CVCL_0570) constitutively expressing Cas9 (Gandhi et al., 2017) were cultured in DMEM (Corning) supplemented with 10% fetal bovine serum (Gibco) and 1% penicillin/streptomycin (Corning) at 37°C and 5% CO_2 in 12-well plates to 80% confluency. For transfection, each well received 2 µl of Lipofectamine 3000 reagent and 2 µl P3000 reagent (Thermo Fisher Scientific) with 1 µg of cU6.3(LTK.20). Transfected cells were cultured for 48 h, trypsinized and genomic DNA was harvested with the DNeasy Blood and Tissue kit (QIAGEN). A 1.2 kb region around the LTK.20 target was PCR-amplified with the primers LTK-F2/LTK-R2 and the product was ligated into pGEM-T (Promega) for Sanger sequencing genotyping of 12 individual clones. For midkine, a gRNA targeted to exon 1 (MK.1: GAGGCTGCCAAAGCCAAGAA) was synthesized *in vitro*, together with a standard control gRNA (Talbot and Amacher, 2014). EnGen Cas9 protein (New England Biolabs) was complexed with equimolar quantities of purified gRNA for 15 min at 37°C and diluted to 0.5 µg/µl for electroporation into HH5-6 embryos (Hutchins and Bronner, 2018).

Plasmid constructs

To create pCAG(V5-LTK), pCAG(V5-LTK-isoform2), pCAG(V5-LTK-ΔICD) and pCAG(V5-LTK-ΔECD), the signal peptide and the remaining full-length or truncated sequences of LTK were PCR amplified from stage HH 10 cDNA with the primer pairs pCAG-LTK-F/V5-LTK-R and V5-LTK-F/pCAG-LTK-R (full-length) or V5-LTK-F/pCAG-LTK-R2 (-ΔICD), or pCAG-LTK-F/V5-LTK-R2 and V5-LTK-F2/pCAG-LTK-R (-ΔECD) (Table S1), and ligated using Gibson Assembly (NEB) into the backbone of pCI-H2B-RFP (Betancur et al., 2010) digested with *Eco*RI and *Not*I (to remove IRES and H2B-RFP). To create pCI-H2B-RFP(V5-LTK-ΔICD), the coding sequence for the carboxyl terminus up to residue R880 was amplified with the primer pair V5-LTK-F/pCI-LTK-R2 (Table S1) and Gibson assembled with the signal peptide sequence into pCI-H2B-RFP digested with *Eco*RV. To create pCI-H2B-RFP(midkine-FLAG), pCI-H2B-RFP(midkine-ΔSP-FLAG) and pCI-GFP(midkine-FLAG), full-length or truncated midkine sequences lacking a stop codon were PCR-amplified with the primers pCI-MK-F/MK-R or pCI-MK-F2/MK-R, and Gibson assembled with the single-strand oligos FLAG-MK-R and FLAG-pCI-F (Table S1) into pCI-H2B-RFP or pCI-GFP (Megason and McMahon, 2002) digested with *Cla*I and *Sma*I. Sanger sequencing was used to confirm integrity of clones used for transfection.

Pharmacological inhibitor treatments

The right-side head mesenchyme of stage HH9 embryos was injected *in ovo* with Ringer's solution containing 100 µM ceritinib (Selleck Chemicals, S7083) or 100 µM crizotinib (Sigma-Aldrich, PZ0191) ALK inhibitors, prepared from 10 mM stocks diluted in DMSO; Ringer's solution with 1% DMSO was injected into the left-side mesenchyme as a contralateral control. The eggs were closed and re-incubated for 5 h at 37°C.

Culture of cranial neural fold explants

Stage HH5 embryos were electroporated *ex ovo* with control gRNA on the left side and LTK.20 gRNA on the right side and cultured to 5-6 somites. The neural folds were dissected in Ringer's solution and transferred into wells of fibronectin-coated glass chamber slides (LabTek) containing 200 µl of 10% horse serum/15% embryo in Modified Eagle's Medium (Bronner-Fraser and García-Castro, 2008). After 1 h, 200 µl the same medium were added and the explants were cultured for 24 h at 37°C and 5% CO_2. The cultured explants were fixed in 4% paraformaldehyde (PFA) for 20 min and processed for immunostaining, followed by mounting in Fluoromount (Southern Biotech) and imaging with an Axiocam 506 mono camera and an Apotome.2 microscope (Zeiss).

In situ hybridization

Stage HH4 to HH 20 embryos were fixed overnight in 4% PFA in PBS at 4°C. Fixed embryos were washed and dissected in dyethil pyrocarbonate-treated PBS+0.1% Tween-20 (PBST), dehydrated in a methanol/PBS series and stored in methanol at −20°C. Rehydrated embryos were hybridized as whole-mount embryos at 68-70°C (Wilkinson, 1992; Simões-Costa et al., 2015). Colorimetric signal was developed with NBT-BCIP substrates (Roche), followed by fixing in 4% PFA in PBS and serial dehydration and rehydration in methanol before imaging. Templates for *LTK* (Simões-Costa et al., 2014) and *Sox10* (Betancur et al., 2010) probes were described previously. A template for midkine probe was PCR-amplified with the primers MK-F1 and MK-R1 (Table S1) and cloned into pGEM-T vector (Promega). Template DNA was linearized using unique restriction sites 5′ to the insert, purified and transcribed with digoxigenin-labeled nucleotides (Roche). Synthesized probes were purified using Illustra ProbeQuant G-50 Micro Columns (GE Healthcare).

Immunohistochemistry

Stage HH8 to HH10 embryos were fixed for 15-20 min in 4% PFA in 0.1 M phosphate buffer, pH 7.4, at room temperature. Fluorescent immunostaining was performed in whole mounts as described (Ezin et al., 2009). The embryos were permeabilized with 0.5% Triton X-100 in PBS (PBT). Blocking was performed with 10% goat or donkey serum in PBT for 1-3 h and antibodies were diluted in the same blocking solution. Primary antibodies used were: mouse IgM anti-HNK-1 (DSHB, 3H5, RRID: AB_2314644; 1:5), goat IgG anti-fluorescein (Novus, NB600-493, RRID: AB_10001854; 1:500), mouse IgG1 anti-Pax7 (DSHB, pax7, RRID: AB_528428; 1:5), rabbit IgG anti-cleaved caspase 3 (R&D Systems, AF835, RRID:AB_2243952; 1:500), rabbit IgG anti-Sox9 (Millipore,

Development (2018) 145, dev164046. doi:10.1242/dev.164046

AB5535, RRID:AB_2239761, 1:500), rabbit IgG anti-midkine (Abcam, ab52637, RRID:AB_880698, 1:500), mouse IgG2a anti-V5 (Thermo Fisher Scientific, R960-25, RRID:AB_2556564, 1:500), mouse IgG2a anti-Ecad (BD Biosciences, 610181, RRID:AB_397580, 1:1000), mouse IgG1 anti-FLAG M2 (Sigma-Aldrich, F1804, RRID:AB_262044, 1:500). Secondary antibodies used were: goat anti-mouse IgM Alexa 488/568, goat anti-mouse IgG1 488/647, goat anti-mouse IgG2a 350/488, goat anti-rabbit IgG Alexa 488/647 (Molecular Probes; 1:500 for Alexa 350/647 and 1:100 for Alexa 488/568). Images were captured with an Axiocam 506 mono camera and an Apotome.2 microscope (Zeiss), and Zen Blue software (Zeiss) was used to create maximum intensity projections and perform gamma adjustments.

Histology

Embryos were cryoprotected by incubation for several hours in PBS containing 5% then 15% sucrose, at 4°C. Protected embryos were equilibrated in 7.5% gelatin/15% sucrose in 0.5× PBS at 37°C for 3-8 h and mounted at room temperature. The blocks were snap-frozen in liquid nitrogen and stored at −80°C. Sections of 12-14 µm (immunofluorescence) or 20-25 µm (*in situ* hybridization) were obtained using a Microm HM550 cryostat (Thermo Fisher Scientific) and collected on Super Frost Plus slides (Thermo Fisher Scientific), let dry for at least 10 min and mounted in Fluoromount (Southern Biotech) after gelatin removal in a 37°C bath for 15-20 min.

Proximity ligation assay (PLA)

Stage HH5 embryos were co-electroporated *ex ovo* with 2.5 µg/µl pCAG(V5-LTK), pCAG(V5-LTK-isoform2), pCAG(V5-LTK-ΔECD) or pCAG(V5-LTK-ΔICD) and/or 1 µg/µl pCI-H2B-RFP reporter, cultured to stage HH10 and fixed for 20 min in 4% PFA in 0.1 M PB before embedding and sectioning. The area containing 12-14 sections on SuperFrost slides was delimited with a hydrophobic pen before gelatin removal. The sections were permeabilized with 0.1% Triton X-100 in PBS and blocked with 10% donkey serum in PBST. Primary antibody incubation was performed overnight at 4°C with rabbit IgG anti-midkine (Abcam, ab52637, RRID: AB_880698, 1:500) and mouse IgG2a anti-V5 (Thermo Fisher Scientific, R960-25, RRID:AB_2556564, 1:500) diluted in blocking solution. Duolink PLA probes (Sigma) were diluted in the same blocking solution and green Duolink Fluorescent Detection Reagent (Sigma) was used to generate signal according to the manufacturer's instructions.

Quantification and statistical analysis

To quantify the neural crest area, dorsal view micrographs were used to delimit and measure the $Pax7^+$, $Snail2^+$ or $Sox9^+$ field of each side of a HH9+ embryo head. To count $Sox9^+$ cells, stained nuclei on each side of 14-18 transverse non-consecutive sections of five embryos were identified and measured with the tool Analyze Particles in Fiji (Schindelin et al., 2012). PLA puncta in the dorsal region in 14 sections of two embryos were manually counted. Statistical significance was determined with a two-tailed paired *t*-test.

Immunoprecipitation

NIH/3T3 mouse embryonic fibroblasts (ATCC, CRL-1658, RRID: CVCL_0594) in DMEM (Corning) supplemented with 10% fetal bovine serum (Gibco) and 1% penicillin/streptomycin (Corning) were cultured at 37°C and 5% CO_2 in 100 mm plates to 70% confluency. Transfection was performed using Lipofectamine 3000 (Invitrogen). Each well received 30 µl of Lipofectamine 3000 reagent and 30 µl P3000 reagent with 10 µg of pCAG(V5-LTK) and 7 µg of pCI-GFP(midkine-FLAG) or pCI-GFP. Transfected cells were cultured for 24 h and lysed for 30 min in 1 ml of 150 mM NaCl/50 mM Tris pH 7.4/1% NP-40 buffer at 4°C. Lysates were cleared by centrifugation (15 min at 20,000 ***g***) at 4°C and pre-incubation with protein-G agarose for 15 min at 4°C. 500 µl of pre-cleared lysates were immunoprecipitated by protein-G agarose beads coated with 6 µg mouse IgG1 anti-FLAG M2 (Sigma-Aldrich, F1804, RRID: AB_262044) for 8 h at 4°C.

Western blotting

Input (20-30 µg) and immunoprecipitated samples or 10 µg of protein from HH10 embryos lysed in 8 M urea/2.5% SDS for 15 min at 65°C were loaded and separated in a Bolt 4-12% Bis-Tris Plus gel (Thermo Fisher Scientific). Transfer to nitrocellulose membrane was performed at 100 V for 1 h at 4°C in 25 mM Tris/0.2 M glycine/20% methanol buffer. The membrane was blocked with 5% bovine serum albumin and 0.1% Tween-20 in Tris-buffered saline (TBST), pH 7.6 for 1 h and incubated with primary antibodies rabbit mouse IgG2a anti-V5 (Thermo Fisher Scientific, R960-25, RRID:AB_2556564, 1:2000) and mouse IgG1 anti-FLAG M2 (Sigma-Aldrich, F1804, RRID:AB_262044, 1:500) or IgG anti-midkine (Abcam, ab52637, RRID:AB_880698, 1:1000) diluted in blocking solution overnight at 4°C. Secondary antibody incubation was performed with goat peroxidase-labeled anti-mouse IgG (KPL, 74-1806; 1:10,000) or anti-rabbit IgG (KPL, 74-1506; 1:25,000) in 5% milk in TBST for 1 h. Post-primary and secondary antibody washes were performed in TBST. For radiographic detection, chemiluminescence was developed with the ECL Western Blotting System (GE Healthcare).

Acknowledgements

We thank Marcos Simões-Costa and Stephen Roberts for kindly sharing reagents, Narmada Thayapran for technical assistance, and Yuwei Li for valuable comments on the manuscript.

Competing interests

The authors declare no competing or financial interests.

Author contributions

Conceptualization: F.M.V., M.E.B.; Methodology: F.M.V.; Formal analysis: F.M.V.; Investigation: F.M.V.; Data curation: F.M.V.; Writing - original draft: F.M.V., M.E.B.; Writing - review & editing: F.M.V., M.E.B.; Visualization: F.M.V.; Supervision: M.E.B.; Funding acquisition: F.M.V., M.E.B.

Funding

This work was supported by a National Institutes of Health grant (R01DE024157 to M.E.B.) and postdoctoral fellowships from the Brazilian National Council for Scientific and Technological Development (Conselho Nacional de Desenvolvimento Científico e Tecnológico) (CNPq PDE 207656/2014-2 to F.M.V.) and the Shurl and Kay Curci Foundation (to F.M.V.). Deposited in PMC for release after 12 months.

Supplementary information

Supplementary information available online at
http://dev.biologists.org/lookup/doi/10.1242/dev.164046.supplemental

References

Acloque, H., Adams, M. S., Fishwick, K., Bronner-Fraser, M. and Nieto, M. A. (2009). Epithelial-mesenchymal transitions: the importance of changing cell state in development and disease. *J. Clin. Invest.* **119**, 1438-1449.

Ahlgren, S. C. and Bronner-Fraser, M. (1999). Inhibition of Sonic hedgehog signaling in vivo results in craniofacial neural crest cell death. *Curr. Biol.* **9**, 1304-1314.

Amaya, E., Musci, T. J. and Kirschner, M. W. (1991). Expression of a dominant negative mutant of the FGF receptor disrupts mesoderm formation in xenopus embryos. *Cell* **66**, 257-270.

Bahm, I., Barriga, E. H., Frolov, A., Theveneau, E., Frankel, P. and Mayor, R. (2017). PDGF controls contact inhibition of locomotion by regulating N-cadherin during neural crest migration. *Development* **144**, 2456-2468.

Baker, C. V., Bronner-Fraser, M., Le Douarin, N. M. and Teillet, M. A. (1997). Early- and late-migrating cranial neural crest cell populations have equivalent developmental potential in vivo. *Development* **124**, 3077-3087.

Barrallo-Gimeno, A., Holzschuh, J., Driever, W. and Knapik, E. W. (2004). Neural crest survival and differentiation in zebrafish depends on mont blanc/tfap2a gene function. *Development* **131**, 1463-1477.

Ben-Neriah, Y. and Bauskin, A. R. (1988). Leukocytes express a novel gene encoding a putative transmembrane protein-kinase devoid of an extracellular domain. *Nature* **333**, 672-676.

Betancur, P., Bronner-Fraser, M. and Sauka-Spengler, T. (2010). Genomic code for Sox10 activation reveals a key regulatory enhancer for cranial neural crest. *Proc. Natl. Acad. Sci. USA* **107**, 3570-3575.

Bronner-Fraser, M. and García-Castro, M. (2008). Chapter 4 manipulations of neural crest cells or their migratory pathways. *Methods Cell Biol.* **87**, 75-96.

Chapman, S. C., Collignon, J., Schoenwolf, G. C. and Lumsden, A. (2001). Improved method for chick whole-embryo culture using a filter paper carrier. *Dev. Dyn.* **220**, 284-289.

Cheung, M., Chaboissier, M.-C., Mynett, A., Hirst, E., Schedl, A. and Briscoe, J. (2005). The transcriptional control of trunk neural crest induction, survival, and delamination. *Dev. Cell* **8**, 179-192.

Coles, E. G., Taneyhill, L. A. and Bronner-Fraser, M. (2007). A critical role for Cadherin6B in regulating avian neural crest emigration. *Dev. Biol.* **312**, 533-544.
Dirks, W. G., Fähnrich, S., Lis, Y., Becker, E., MacLeod, R. A. F. and Drexler, H. G. (2002). Expression and functional analysis of the anaplastic lymphoma kinase (ALK) gene in tumor cell lines. *Int. J. Cancer* **100**, 49-56.
Dottori, M., Gross, M. K., Labosky, P. and Goulding, M. (2001). The winged-helix transcription factor Foxd3 suppresses interneuron differentiation and promotes neural crest cell fate. *Development* **128**, 4127-4138.
Ezin, A. M., Fraser, S. E. and Bronner-Fraser, M. (2009). Fate map and morphogenesis of presumptive neural crest and dorsal neural tube. *Dev. Biol.* **330**, 221-236.
Fadeev, A., Krauss, J., Singh, A. P. and Nüsslein-Volhard, C. (2016). Zebrafish Leucocyte tyrosine kinase controls iridophore establishment, proliferation and survival. *Pigment Cell Melanoma Res.* **29**, 284-296.
Fadeev, A., Mendoza-Garcia, P., Irion, U., Guan, J., Pfeifer, K., Wiessner, S., Serluca, F., Singh, A. P., Nüsslein-Volhard, C. and Palmer, R. H. (2018). ALKALs are in vivo ligands for ALK family receptor tyrosine kinases in the neural crest and derived cells. *Proc. Natl. Acad. Sci. USA* **115**, E630-E638.
Fairchild, C. L. and Gammill, L. S. (2013). Tetraspanin18 is a FoxD3-responsive antagonist of cranial neural crest epithelial-to-mesenchymal transition that maintains cadherin-6B protein. *J. Cell Sci.* **126**, 1464-1476.
Frisch, S. M. and Francis, H. (1994). Disruption of epithelial cell-matrix interactions induces apoptosis. *J. Cell Biol.* **124**, 619-626.
Gammill, L. S., Gonzalez, C. and Bronner-Fraser, M. (2007). Neuropilin 2/semaphorin 3F signaling is essential for cranial neural crest migration and trigeminal ganglion condensation. *Dev. Neurobiol.* **67**, 47-56.
Gandhi, S., Piacentino, M. L., Vieceli, F. M. and Bronner, M. E. (2017). Optimization of CRISPR/Cas9 genome editing for loss-of-function in the early chick embryo. *Dev. Biol.* **432**, 86-97.
Green, S. A., Simoes-Costa, M. and Bronner, M. E. (2015). Evolution of vertebrates as viewed from the crest. *Nature* **520**, 474-482.
Guan, J., Umapathy, G., Yamazaki, Y., Wolfstetter, G., Mendoza, P., Pfeifer, K., Mohammed, A., Hugosson, F., Zhang, H., Hsu, A. W. et al. (2015). FAM150A and FAM150B are activating ligands for anaplastic lymphoma kinase. *eLife* **4**, e09811.
Hamburger, V. and Hamilton, H. L. (1951). A series of normal stages in the development of the chick embryo. *J. Morphol.* **88**, 49-92.
Honoré, S. M., Aybar, M. J. and Mayor, R. (2003). Sox10 is required for the early development of the prospective neural crest in Xenopus embryos. *Dev. Biol.* **260**, 79-96.
Huang, C., Kratzer, M.-C., Wedlich, D. and Kashef, J. (2016). E-cadherin is required for cranial neural crest migration in Xenopus laevis. *Dev. Biol.* **411**, 159-171.
Hugosson, F., Sjögren, C., Birve, A., Hedlund, L., Eriksson, T. and Palmer, R. H. (2014). The Drosophila midkine/Pleiotrophin homologues Miple1 and Miple2 affect adult lifespan but are dispensable for Alk signaling during embryonic gut formation. *PLoS ONE* **9**, e112250.
Hurley, S. P., Clary, D. O., Copie, V. and Lefcort, F. (2006). Anaplastic lymphoma kinase is dynamically expressed on subsets of motor neurons and in the peripheral nervous system. *J. Comp. Neurol.* **495**, 202-212.
Hutchins, E. J. and Bronner, M. E. (2018). Draxin acts as a molecular rheostat of canonical Wnt signaling to control cranial neural crest EMT. *J. Cell Biol.* (in press).
Itasaki, N., Bel-Vialar, S. and Krumlauf, R. (1999). 'Shocking' developments in chick embryology: electroporation and in ovo gene expression. *Nat. Cell Biol.* **1**, E203-E207.
Jeong, J., Mao, J., Tenzen, T., Kottmann, A. H. and McMahon, A. P. (2004). Hedgehog signaling in the neural crest cells regulates the patterning and growth of facial primordia. *Genes Dev.* **18**, 937-951.
Kadomatsu, K. and Muramatsu, T. (2004). Midkine and pleiotrophin in neural development and cancer. *Cancer Lett.* **204**, 127-143.
Kam, M. K. M., Cheung, M. C. H., Zhu, J. J., Cheng, W. W. C., Sat, E. W. Y., Tam, P. K. H. and Lui, V. C. H. (2014). Perturbation of Hoxb5 signaling in vagal and trunk neural crest cells causes apoptosis and neurocristopathies in mice. *Cell Death Differ.* **21**, 278-289.
Kashef, J., Köhler, A., Kuriyama, S., Alfandari, D., Mayor, R. and Wedlich, D. (2009). Cadherin-11 regulates protrusive activity in Xenopus cranial neural crest cells upstream of Trio and the small GTPases. *Genes Dev.* **23**, 1393-1398.
Kee, Y. and Bronner-Fraser, M. (2005). To proliferate or to die: role of Id3 in cell cycle progression and survival of neural crest progenitors. *Genes Dev.* **19**, 744-755.
Kerosuo, L. and Bronner-Fraser, M. (2012). What is bad in cancer is good in the embryo: importance of EMT in neural crest development. *Semin. Cell Dev. Biol.* **23**, 320-332.
Kosicki, M., Tomberg, K. and Bradley, A. (2018). Repair of double-strand breaks induced by CRISPR/Cas9 leads to large deletions and complex rearrangements. *Nat. Biotechnol.* **36**, 765-771.
Kramer, M., Ribeiro, D., Arsenian-Henriksson, M., Deller, T. and Rohrer, H. (2016). Proliferation and survival of embryonic sympathetic neuroblasts by MYCN and activated ALK signaling. *J. Neurosci.* **36**, 10425-10439.
Kulesa, P. M. and Gammill, L. S. (2010). Neural crest migration: patterns, phases and signals. *Dev. Biol.* **344**, 566-568.
Kulesa, P. M., Bailey, C. M., Kasemeier-Kulesa, J. C. and McLennan, R. (2010). Cranial neural crest migration: new rules for an old road. *Dev. Biol.* **344**, 543-554.
Le Douarin, N. and Kalcheim, C. (1999). *The Neural Crest*. Cambridge, UK: Cambridge University Press.
Lee, H.-H., Norris, A., Weiss, J. B. and Frasch, M. (2003). Jelly belly protein activates the receptor tyrosine kinase Alk to specify visceral muscle pioneers. *Nature* **425**, 507-512.
Light, W., Vernon, A. E., Lasorella, A., Iavarone, A. and LaBonne, C. (2005). Xenopus Id3 is required downstream of Myc for the formation of multipotent neural crest progenitor cells. *Development* **132**, 1831-1841.
Lopes, S. S., Yang, X., Müller, J., Carney, T. J., McAdow, A. R., Rauch, G.-J., Jacoby, A. S., Hurst, L. D., Delfino-Machín, M., Haffter, P. et al. (2008). Leukocyte tyrosine kinase functions in pigment cell development. *PLoS Genet.* **4**, e1000026.
Lorente, M., Torres, S., Salazar, M., Carracedo, A., Hernández-Tiedra, S., Rodríguez-Fornés, F., García-Taboada, E., Meléndez, B., Mollejo, M., Campos-Martín, Y. et al. (2011a). Stimulation of the midkine/ALK axis renders glioma cells resistant to cannabinoid antitumoral action. *Cell Death Differ.* **18**, 959-973.
Lorente, M., Torres, S., Salazar, M., Carracedo, A., Hernández-Tiedra, S., Rodríguez-Fornés, F., García-Taboada, E., Meléndez, B., Mollejo, M., Campos-Martín, Y. et al. (2011b). Stimulation of ALK by the growth factor midkine renders glioma cells resistant to autophagy-mediated cell death. *Autophagy* **7**, 1071-1073.
Marmor, M. D. and Yarden, Y. (2004). Role of protein ubiquitylation in regulating endocytosis of receptor tyrosine kinases. *Oncogene* **23**, 2057-2070.
Mathivet, T., Mazot, P. and Vigny, M. (2007). In contrast to agonist monoclonal antibodies, both C-terminal truncated form and full length form of Pleiotrophin failed to activate vertebrate ALK (anaplastic lymphoma kinase). *Cell. Signal.* **19**, 2434-2443.
McLennan, R., Teddy, J. M., Kasemeier-Kulesa, J. C., Romine, M. H. and Kulesa, P. M. (2010). Vascular endothelial growth factor (VEGF) regulates cranial neural crest migration in vivo. *Dev. Biol.* **339**, 114-125.
Megason, S. G. and McMahon, A. P. (2002). A mitogen gradient of dorsal midline Wnts organizes growth in the CNS. *Development* **129**, 2087-2098.
Miyake, I., Hakomori, Y., Shinohara, A., Gamou, T., Saito, M., Iwamatsu, A. and Sakai, R. (2002). Activation of anaplastic lymphoma kinase is responsible for hyperphosphorylation of ShcC in neuroblastoma cell lines. *Oncogene* **21**, 5823-5834.
Mo, E. S., Cheng, Q., Reshetnyak, A. V., Schlessinger, J. and Nicoli, S. (2017). Alk and Ltk ligands are essential for iridophore development in zebrafish mediated by the receptor tyrosine kinase Ltk. *Proc. Natl. Acad. Sci. USA* **114**, 12027-12032.
Moog-Lutz, C., Degoutin, J., Gouzi, J. Y., Frobert, Y., Carvalho, N. B.-D., Bureau, J., Créminon, C. and Vigny, M. (2005). Activation and inhibition of anaplastic lymphoma kinase receptor tyrosine kinase by monoclonal antibodies and absence of agonist activity of pleiotrophin. *J. Biol. Chem.* **280**, 26039-26048.
Motegi, A., Fujimoto, J., Kotani, M., Sakuraba, H. and Yamamoto, T. (2004). ALK receptor tyrosine kinase promotes cell growth and neurite outgrowth. *J. Cell Sci.* **117**, 3319-3329.
Mourali, J., Benard, A., Lourenco, F. C., Monnet, C., Greenland, C., Moog-Lutz, C., Racaud-Sultan, C., Gonzalez-Dunia, D., Vigny, M., Mehlen, P. et al. (2006). Anaplastic lymphoma kinase is a dependence receptor whose proapoptotic functions are activated by caspase cleavage. *Mol. Cell. Biol.* **26**, 6209-6222.
Müller-Tidow, C., Diederichs, S., Bulk, E., Pohle, T., Steffen, B., Schwäble, J., Plewka, S., Thomas, M., Metzger, R., Schneider, P. M. et al. (2005). Identification of metastasis-associated receptor tyrosine kinases in non-small cell lung cancer. *Cancer Res.* **65**, 1778-1782.
Muramatsu, T. (2010). Midkine, a heparin-binding cytokine with multiple roles in development, repair and diseases. *Proc. Jpn. Acad. Ser. B* **86**, 410-425.
Nieto, M. A. (2002). The snail superfamily of zinc-finger transcription factors. *Nat. Rev. Mol. Cell Biol.* **3**, 155-166.
Nieto, M. A., Sargent, M. G., Wilkinson, D. G. and Cooke, J. (1994). Control of cell behavior during vertebrate development by Slug, a zinc finger gene. *Science* **264**, 835-839.
Olesnicky Killian, E. C., Birkholz, D. A. and Artinger, K. B. (2009). A role for chemokine signaling in neural crest cell migration and craniofacial development. *Dev. Biol.* **333**, 161-172.
Osborne, N. J., Begbie, J., Chilton, J. K., Schmidt, H. and Eickholt, B. J. (2005). Semaphorin/neuropilin signaling influences the positioning of migratory neural crest cells within the hindbrain region of the chick. *Dev. Dyn.* **232**, 939-949.
Qi, M., Ikematsu, S., Ichihara-Tanaka, K., Sakuma, S., Muramatsu, T. and Kadomatsu, K. (2000). Midkine rescues Wilms, tumor cells from cisplatin-induced apoptosis: regulation of Bcl-2 expression by Midkine. *J. Biochem.* **127**, 269-277.

Reiff, T., Huber, L., Kramer, M., Delattre, O., Janoueix-Lerosey, I. and Rohrer, H. (2011). Midkine and Alk signaling in sympathetic neuron proliferation and neuroblastoma predisposition. *Development* **138**, 4699-4708.

Reshetnyak, A. V., Murray, P. B., Shi, X., Mo, E. S., Mohanty, J., Tome, F., Bai, H., Gunel, M., Lax, I. and Schlessinger, J. (2015). Augmentor α and β (FAM150) are ligands of the receptor tyrosine kinases ALK and LTK: hierarchy and specificity of ligand–receptor interactions. *Proc. Natl. Acad. Sci. USA* **112**, 15862-15867.

Rodrigues, F. S. L. M., Yang, X., Nikaido, M., Liu, Q. and Kelsh, R. N. (2012). A simple, highly visual in vivo screen for anaplastic lymphoma kinase inhibitors. *ACS Chem. Biol.* **7**, 1968-1974.

Rogers, C. D., Saxena, A. and Bronner, M. E. (2013). Sip1 mediates an E-cadherin-to-N-cadherin switch during cranial neural crest EMT. *J. Cell Biol.* **203**, 835-847.

Rogers, C. D., Sorrells, L. K. and Bronner, M. E. (2018). A catenin-dependent balance between N-cadherin and E-cadherin controls neuroectodermal cell fate choices. *Mech. Dev.* **152**, 44-56.

Roll, J. D. and Reuther, G. W. (2012). ALK-activating homologous mutations in LTK induce cellular transformation. *PLoS ONE* **7**, e31733.

Saffell, J. L., Williams, E. J., Mason, I. J., Walsh, F. S. and Doherty, P. (1997). Expression of a dominant negative FGF receptor inhibits axonal growth and FGF receptor phosphorylation stimulated by CAMs. *Neuron* **18**, 231-242.

Sauka-Spengler, T. and Barembaum, M. (2008). Chapter 12 gain- and loss-of-function approaches in the chick embryo. *Methods Cell Biol.* **87**, 237-256.

Scarpa, E., Szabó, A., Bibonne, A., Theveneau, E., Parsons, M. and Mayor, R. (2015). Cadherin switch during EMT in neural crest cells leads to contact inhibition of locomotion via repolarization of forces. *Dev. Cell* **34**, 421-434.

Schindelin, J., Arganda-Carreras, I., Frise, E., Kaynig, V., Longair, M., Pietzsch, T., Preibisch, S., Rueden, C., Saalfeld, S., Schmid, B. et al. (2012). Fiji: an open-source platform for biological-image analysis. *Nat. Methods* **9**, 676-682.

Schwarz, Q., Vieira, J. M., Howard, B., Eickholt, B. J. and Ruhrberg, C. (2008). Neuropilin 1 and 2 control cranial gangliogenesis and axon guidance through neural crest cells. *Development* **135**, 1605-1613.

Simões-Costa, M., Tan-Cabugao, J., Antoshechkin, I., Sauka-Spengler, T. and Bronner, M. E. (2014). Transcriptome analysis reveals novel players in the cranial neural crest gene regulatory network. *Genome Res.* **24**, 281-290.

Simões-Costa, M., Stone, M. and Bronner, M. E. (2015). Axud1 Integrates Wnt Signaling and Transcriptional Inputs to Drive Neural Crest Formation. *Dev. Cell* **34**, 544-554.

Söderberg, O., Gullberg, M., Jarvius, M., Ridderstråle, K., Leuchowius, K.-J., Jarvius, J., Wester, K., Hydbring, P., Bahram, F., Larsson, L.-G. et al. (2006). Direct observation of individual endogenous protein complexes in situ by proximity ligation. *Nat. Methods* **3**, 995-1000.

Stoica, G. E., Kuo, A., Aigner, A., Sunitha, I., Souttou, B., Malerczyk, C., Caughey, D. J., Wen, D., Karavanov, A., Riegel, A. T. et al. (2001). Identification of anaplastic lymphoma kinase as a receptor for the growth factor pleiotrophin. *J. Biol. Chem.* **276**, 16772-16779.

Stoica, G. E., Kuo, A., Powers, C., Bowden, E. T., Sale, E. B., Riegel, A. T. and Wellstein, A. (2002). Midkine binds to anaplastic lymphoma kinase (ALK) and acts as a growth factor for different cell types. *J. Biol. Chem.* **277**, 35990-35998.

Talbot, J. C. and Amacher, S. L. (2014). A streamlined CRISPR pipeline to reliably generate Zebrafish frameshifting alleles. *Zebrafish* **11**, 583-585.

Taneyhill, L. A. (2008). To adhere or not to adhere: the role of Cadherins in neural crest development. *Cell Adh. Migr.* **2**, 223-230.

Taneyhill, L. A., Coles, E. G. and Bronner-Fraser, M. (2007). Snail2 directly represses cadherin6B during epithelial-to-mesenchymal transitions of the neural crest. *Development* **134**, 1481-1490.

Testaz, S. and Duband, J.-L. (2001). Central role of the α4β1 integrin in the coordination of avian truncal neural crest cell adhesion, migration, and survival. *Dev. Dyn.* **222**, 127-140.

Theveneau, E. and Mayor, R. (2012). Neural crest migration: interplay between chemorepellents, chemoattractants, contact inhibition, epithelial-mesenchymal transition, and collective cell migration. *Wiley Interdiscip. Rev. Dev. Biol.* **1**, 435-445.

Theveneau, E., Marchant, L., Kuriyama, S., Gull, M., Moepps, B., Parsons, M. and Mayor, R. (2010). Collective chemotaxis requires contact-dependent cell polarity. *Dev. Cell* **19**, 39-53.

Thiery, J. P., Acloque, H., Huang, R. Y. J. and Nieto, M. A. (2009). Epithelial-mesenchymal transitions in development and disease. *Cell* **139**, 871-890.

Tong, Y., Mentlein, R., Buhl, R., Hugo, H.-H., Krause, J., Mehdorn, H. M. and Held-Feindt, J. (2007). Overexpression of midkine contributes to anti-apoptotic effects in human meningiomas. *J. Neurochem.* **100**, 1097-1107.

Tríbulo, C., Aybar, M. J., Sánchez, S. S. and Mayor, R. (2004). A balance between the anti-apoptotic activity of Slug and the apoptotic activity of msx1 is required for the proper development of the neural crest. *Dev. Biol.* **275**, 325-342.

Uchikawa, M., Ishida, Y., Takemoto, T., Kamachi, Y. and Kondoh, H. (2003). Functional analysis of chicken Sox2 enhancers highlights an array of diverse regulatory elements that are conserved in mammals. *Dev. Cell* **4**, 509-519.

Ueno, H., Hirano, N., Kozutsumi, H., Sasaki, K., Tanaka, T., Yazaki, Y. and Hirai, H. (1995). An epidermal growth factor receptor-leukocyte tyrosine kinase chimeric receptor generates ligand-dependent growth signals through the Ras signaling pathway. *J. Biol. Chem.* **270**, 20135-20142.

Ueno, H., Sasaki, K., Kozutsumi, H., Miyagawa, K., Mitani, K., Yazaki, Y. and Hirai, H. (1996). Growth and survival signals transmitted via two distinct NPXY motifs within leukocyte tyrosine kinase, an insulin receptor-related tyrosine kinase. *J. Biol. Chem.* **271**, 27707-27714.

Ueno, H., Honda, H., Nakamoto, T., Yamagata, T., Sasaki, K., Miyagawa, K., Mitani, K., Yazaki, Y. and Hirai, H. (1997). The phosphatidylinositol 3′ kinase pathway is required for the survival signal of leukocyte tyrosine kinase. *Oncogene* **14**, 3067-3072.

Vallin, J., Girault, J.-M., Thiery, J. P. and Broders, F. (1998). Xenopus cadherin-11 is expressed in different populations of migrating neural crest cells. *Mech. Dev.* **75**, 171-174.

Vega, S., Morales, A. V., Ocaña, O. H., Valdés, F., Fabregat, I. and Nieto, M. A. (2004). Snail blocks the cell cycle and confers resistance to cell death. *Genes Dev.* **18**, 1131-1143.

Weiss, J. B., Suyama, K. L., Lee, H.-H. and Scott, M. P. (2001). Jelly belly: a Drosophila LDL receptor repeat-containing signal required for mesoderm migration and differentiation. *Cell* **107**, 387-398.

Wilkinson, D. G. (1992). *In situ Hybridization: A Practical Approach*. Oxford, UK: IRL Press at Oxford University Press.

Winkler, C. and Moon, R. T. (2001). Zebrafish mdk2, a novel secreted midkine, participates in posterior neurogenesis. *Dev. Biol.* **229**, 102-118.

Winkler, C., Schäfer, M., Duschl, J., Schartl, M. and Volff, J. N. (2003). Functional divergence of two zebrafish midkine growth factors following fish-specific gene duplication. *Genome Res.* **13**, 1067-1081.

Yao, X., Tan, Z., Gu, B., Wu, R.-R., Liu, Y.-K., Dai, L.-C. and Zhang, M. (2010). Promotion of self-renewal of embryonic stem cells by midkine. *Acta Pharmacol. Sin.* **31**, 629-637.

Zhang, H., Pao, L. I., Zhou, A., Brace, A. D., Halenbeck, R., Hsu, A. W., Bray, T. L., Hestir, K., Bosch, E., Lee, E. et al. (2014). Deorphanization of the human leukocyte tyrosine kinase (LTK) receptor by a signaling screen of the extracellular proteome. *Proc. Natl. Acad. Sci. USA* **111**, 15741-15745.

Zou, P., Muramatsu, H., Miyata, T. and Muramatsu, T. (2006). Midkine, a heparin-binding growth factor, is expressed in neural precursor cells and promotes their growth. *J. Neurochem.* **99**, 1470-1479.